Assessing sustainability potential of alkali-activated concrete from electric arc furnace slag using the ECO_2 framework

Hisham Hafez[1], Dany Kassim[2], Rawaz Kurda[3,4], Rui Vasco Silva[2], Jorge de Brito[2]

[1] Department of Mechanical and Construction Engineering, Northumbria University, Newcastle, UK, hisham.hafez@northumbria.ac.uk (H.H.)

[2] CERIS, Instituto Superior Técnico, Universidade de Lisboa, Portugal, rui.v.silva@tecnico.ulisboa.pt (R.V.S.), jb@civil.ist.utl.pt (J.d.B.)

[3] Department of Highway and Bridge Engineering, Technical Engineering College, Erbil Polytechnic University, Erbil 44001, Iraq, rawaz.kurda@tecnico.ulisboa.pt (R.K.)

[4] Scientific Research and Development Center, Nawroz University, Duhok 42001, Iraq

Abstract

Alkali-activated materials are regarded as a potential sustainable building material with industrial by-products fully replacing ordinary Portland cement. Five million tonnes of electric arc furnace slag are produced annually mostly to be recycled as low value aggregates in several construction applications. This study examined the possibility of valorising the understudied slag as a precursor in alkali-activated concrete. The material, supplied free and available in abundance as a waste, presents a significant potential to produce sustainable concrete. Hence, the mechanical and durability properties of electric arc furnace slag-based alkali-activated concrete were examined. After that, using a sustainability assessment framework called ECO_2, the combined whole-life cycle assessment of the environmental and economic impact was calculated for several mixes that combined electric arc furnace slag and fly ash as precursors. The increasing amount of slag content led to a decline in mechanical performance, though there was an equivalent durability-related performance; mixes with electric arc furnace slag showed equivalent slump and resistance to carbonation, and enhanced resistance to chloride ion penetration. Furthermore, slag-based concrete exhibited significant improvement in the overall ECO_2 sustainability score due to its minimal environmental and economic impact.

Keywords: Sustainability; life cycle assessment; sustainable concrete; electric arc furnace slag; alkali-activated concrete; CO_2.

1. Introduction

Around 30 billion tonnes of conventional concrete were produced in 2015 [1]. Due to its inherent strength and durability properties, concrete is the second most used substance on Earth after water [2]. The use of concrete is associated with immense negative environmental impacts. The current annual production of more than 4 billion tonnes of ordinary Portland cement (OPC) is responsible for 7% of the global CO_2 emissions [3]. Concrete has an environmental impact of 300 kg eq CO_2/m^3 on average, of which 90% is attributable to OPC [4]. Although this is less than that of steel and most polymers per unit mass [5], the intensive use of OPC concrete results in alarming environmental hazards. In China, for example, concrete production alone resulted in approximately 1.5 billion tonnes of greenhouse gas (GHG) emissions in 2014 [6], which represents around 20% of the total produced in the same year [7]. Projections indicate that the growing global urbanization could double the demand of concrete by 2050 [8].

Immense efforts are being made to explore the potential of valorising industrial by-products with low recyclability as precursors of OPC-free binders in alkali-activated concrete (AAC). While an OPC paste is a mixture of Portland cement and water, an AAC mix consists of a precursor and an alkali activator solution. The most well-known activators are sodium hydroxide (SH) and sodium silicate (SS), while fly ash (FA), ground granulated blast furnace slag (GGBS) and calcined clay are recognized precursor types. The strength and durability of an AAC are highly dependent on the quality of the binder, which is determined by three main aspects: 1) the curing method - in Puertas et al. [9] it is argued that dry-sealed curing optimizes the properties of AAC, while in Nasir et al. [10] the significance of heat curing for AAC with several pozzolanic material is emphasized, especially that with FA as a precursor for the first 24 hours; 2) the reactivity of the precursor - the smaller the particle size and the more amorphous the precursor is, the more reactive it is expected to be [11]; 3) the chemical compatibility of the reactants - a precursor is a material with an abundance of either calcium, aluminium or silicon oxide, as shown in Figure 1. It was found that the following four ratios are critical to the functional properties of the AAC mix [12]:

- The mass ratio of solution to the precursor;
- The Si/Al ratio of the chemical composition of the precursor;
- The concentration of the alkali activating solution (Na_2O %);
- The ratio between SiO_2/Na_2O in the alkali activator (MS).

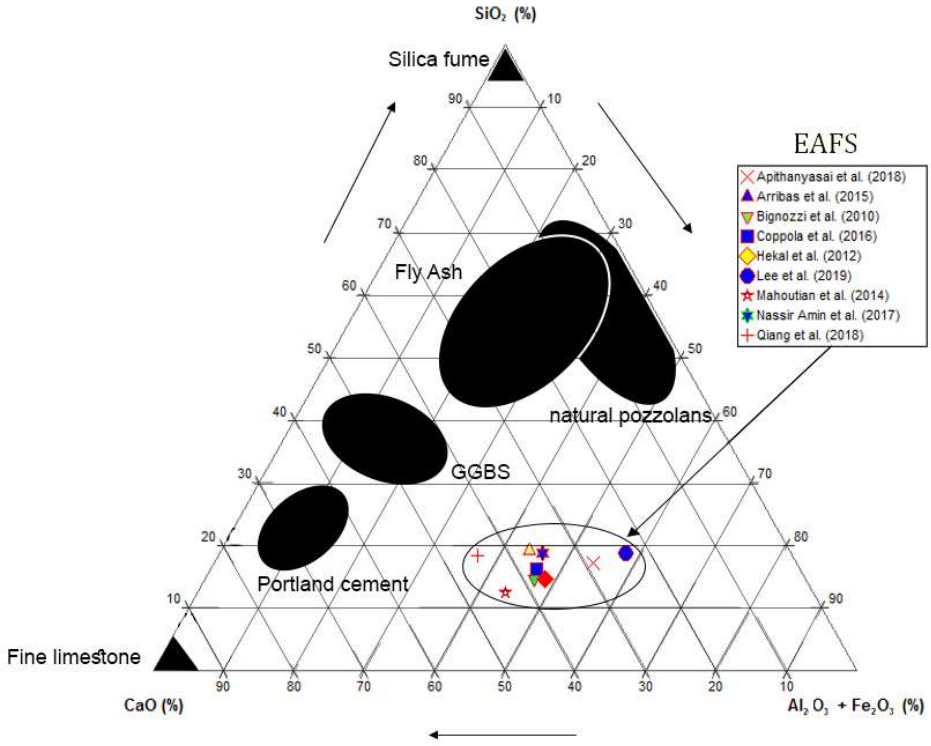

Figure 1: Ternary diagram with the chemical composition of possible precursors for AAC (adapted from Lothenbach et al., 2011 [13])

Most AAC mixes have higher workability than OPC concrete [14], but it is more susceptible to loss after short periods if it presents a high SiO_2/Na_2O ratio. However, AAC is not compatible with most of the commercially available water-reducing agents, which are fundamental to increase the workability beyond a given threshold of the solution to precursor ratio [15]. The compressive strength of an AAC mix can be higher than that of OPC concrete, but the higher the solution concentration (Na_2O %) in a NaOH activator, the higher the strength of the FA-based AAC [16]. Regarding GGBS-based AAC mixes, it was confirmed that the silica modulus is an essential parameter for optimizing the mechanical properties of the resulting AAC [17]. Concerning the resistance to chloride ion penetration, AAC is typically more durable than OPC concrete, but is also highly dependent on the SiO_2/Na_2O ratio in the activator, as well as the ratio of activator/precursor [18]. Finally, it has been established that most AAC mixes are generally less resistant to carbonation than OPC concrete, but are still highly dependent on the optimization of the chemical ratios, as discussed before [19]. Nasir et al. [20-22] observed that admixing 30% slag with the main precursor material, with a 10M solution of NaOH and Na_2SiO_3/NaOH ratio of 2.5, and lower temperature curing favour the densification of the microstructure leading to a reduction in carbonation.

According to Jiang et al. [23], the embodied carbon of an AAC mix is around 50% less than that of an OPC mix. Moreover, industrial by-products are usually cheaper than OPC, which further enhances the sustainability potential of AAC [24]. However, this trend may not be generalized in terms of the environmental and economic impact of all AAC alternatives. The reason is that SS and SH, the main components of the alkaline activator solutions in AAC, are expensive and energy-intensive in production [25]. Another reason is that, in several cases, some energy is required to either prepare the industrial by-product by crushing and milling or when heat curing the AAC [26]. The use of SS and SH also causes a 10-fold increase in human toxicity, ecotoxicity of freshwater bodies and ozone layer depletion potential (ODP) in comparison to conventional OPC-based concrete mixes [4]. However, the ODP impact of 1 kg of cement is insignificant when contextualized to the greater environmental ecosystem since it equals the impact of a household light bulb in a month [27].

Most of the steel production worldwide is shifting towards electric arc furnaces (EAF) because it requires less energy and cost [28]. EAF production technique took over 55% of the market in the US in 2006 [28]. Considering that 50 million tonnes of EAF steel are produced worldwide, around 5 million tonnes of EAFS (~10% of the total amount of EAF steel) are generated in the process [29]. Contrary to GGBS, EAFS are mostly recycled as low-value road embankments [30]. Hence, there is a significant potential for recycling EAFS as a precursor in AAC. In order to assess the suitability of recycling EAFS in binders, the following facts were found in the literature:

- The chemical composition: EAFS mainly consists of 25-40% of iron oxides, 25-40% of calcium oxides, 10-30% of silicon oxides and 5-15% of aluminium oxides (Figure 1). This means that there is abundance in aluminosilicate and EAFS could qualify as a precursor. However, the presence of free CaO provides a threat to its integration in concrete due to risk of volumetric instability [31];
- The physical characterization of EAFS without treatment shows an almost crystalline microstructure, which indicates low reactivity [32]. The reason is that the molten slag is dumped upon formation and is allowed to air cool over a long time.

As received, EAFS is dark in colour, with angular shaped fractions of a hard and rough surface, which makes it adequate for use as an aggregate in concrete [28]. The density of EAFS

varies between 3000 and 3500 kg/m^3, which is 20-30% higher than that of natural aggregates due to the presence of iron and iron oxides [33]. Concrete mixes, in which EAFS was incorporated as coarse aggregates, were found to exhibit lower strength [31]. The higher replacement level of coarse natural aggregates with EAFS, the lower the workability and the higher the shrinkage of concrete [34]. This is because EAFS absorbs 20-30% more water than that of the natural aggregates [35]. Studies showed that integrating EAFS as a partial replacement of OPC up to 20% in blended cement concrete would yield the same compressive strength [36]. For higher replacement ratios, the strength and durability of concrete decreases due to the established low pozzolanic activity [37]. However, further mechanical activation of EAFS; which can be achieved through grinding it to d_{90}=11 micrometres, can increase the replacement ratio up to 30% [38]. The energy required to grind EAFS to the required particle sizes was reported to be 68 kWh/tonne [39]. In addition, re-melting and then quenching of the EAFS could result in a more amorphous microstructure, which would enhance the pozzolanic properties of the slag [40]. However, the initial idea behind recycling EAFS in concrete was to decrease the environmental impact, so special attention is needed when energy-intensive processes are required. When it comes to alkali-activated binders, only a few studies were carried out on the use of EAFS as a precursor in alkali activation [41; 42]. In Apithanyasai et al. [41] an alkaline solution was prepared using 10 M concentration and a silica modulus of 2.5 and the solution/precursor ratio was of 0.9. The compressive strength of the EAFS-based alkali-activated paste was 30% less than that of the control OPC paste but the water absorption and shrinkage were compatible. In addition, Ozturk et al. [42] ran an optimization scheme on several mortar mixes and concluded that the optimum mixes for compressive strengths were obtained when the Na_2O concentration, SiO_2/Na_2O ratio and early age curing temperature were set at 6%, 2 and 80 ◦C, respectively.

There is a clear need for researching the properties of concrete with sustainability potential such as the proposed EAFS-based AAC. As for environmental impacts, although EAFS is a waste and carries minimal impact aside from transportation, processing the slag to increase its reactivity through mechanical activation is an energy intensive process. The same applies to increasing the sodium concentration in the alkali activator to enhance the functional properties of EAFS-based AAC. In terms of economics, EAFS can be supplied for free [41]. This shows sustainability potential in terms of economic and environmental impact when recycled as a precursor for AAC.

However, the functional parameters are still uncertain given the variability in the chemical composition of EAFS and the scarce publications in this regard. FA-based AAC could show satisfactory performance in terms of functional impact depending on the optimized mix design parameters. Therefore, it was decided to use a combination of FA and EAFS as a precursor to produce an optimized mix. Table 1 summarizes the outlines for the optimum mix design from the literature.

Table 1: A summary of the effect of critical parameters of the mix design of AAC on sustainability indicators

Parameter	Interpretation	Action	Predicted effect on the AAC sustainability parameters				
			Functional			Environmental	Economic
			Workability	Strength	Durability		
Particle size of the precursor	Lower sizes increase reactivity	Mechanical activation	NA	⇧	⇧	⬆	⬆
Mineral characteristics of precursor	More amorphous phases increase reactivity	Re-melting and quenching	NA	⇧	⇧	⬆	⬆
Alkalinity of precursor (Kb)	If >1, a base. optimum Ms = 1.00-1.5 If < 1, an acid optimum Ms = 0.75-1.25	The more SS used, the higher the Ms	⬇	⇧	⇧	⬆	⬆
Silica modulus (Ms) = SiO_2/Na_2O	-						
Alkaline concentration (%) = Na_2O	-	The more SH used, he higher the % of sodium oxide in the solution	NA	⇧	⇧	⬆	⬆
Solution: Precursor ratio	Optimum ratio around 0.4	Decrease the ratio	⬇	⇧	⇧	⇩	⇩
EAFS / FA ratio	Replacement (%) of FA by EAFS as a precursor	Increase the ratio	⇧	⇧	⇧	⬆	⬆

Notes: Improvement - ⇧ ⇩; Deterioration - ⬆ ⬇; Not applicable - NA

In a publication of the authors [43], a concrete sustainability assessment framework - ECO_2 - was developed. ECO_2 is primarily a performance-based multi-criteria decision analysis framework that defines sustainability as the user-weighted average of the economic and ecological impact of concrete based on specific functional requirements. The framework as seen in Figure 2, builds on user-defined performance criteria such as minimum slump, strength and a target service life. Based on primary data, the framework performs a life cycle assessment to calculate the environmental and economic impact using parameters such as: global warming potential, ozone layer depletion and net present value of money. The framework, which will be used to assess the sustainability of the studied AAC mixes in this

paper, then calculates he sustainability index, the ECO_2 score, as a weighted average between the aggregated impacts of both pillars.

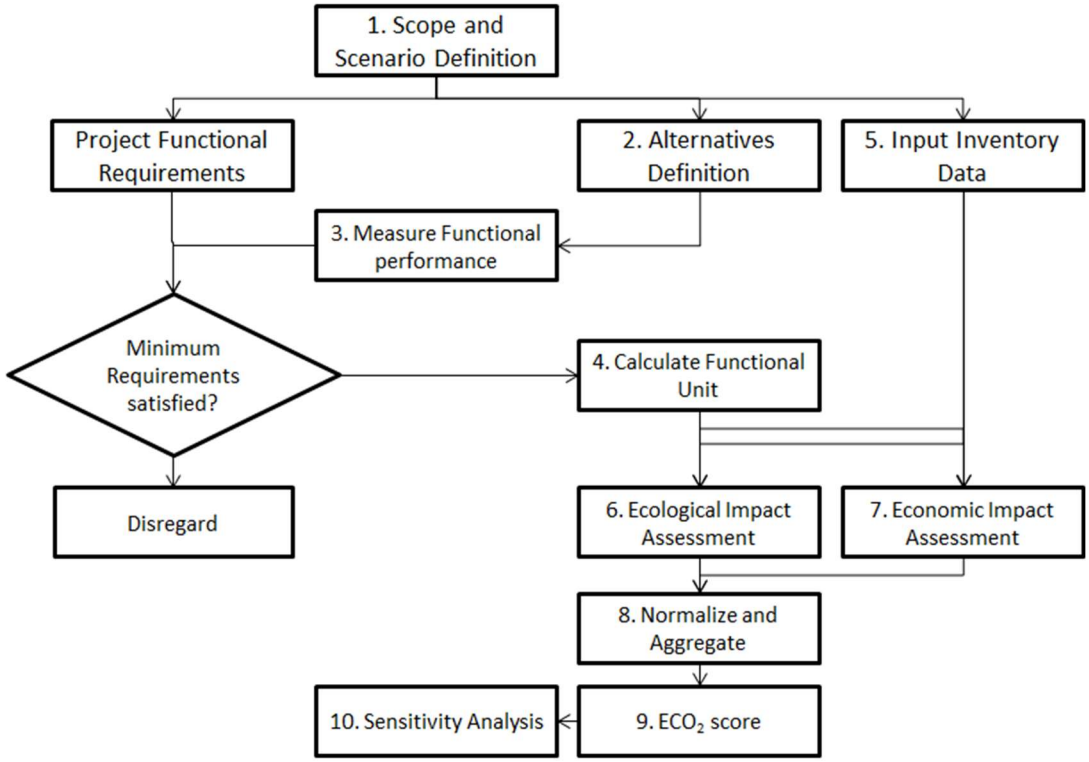

Figure 2: A basic flowchart for the ECO_2 algorithm

2. Materials and methods

2.1 Materials

- Electric arc furnace slag:

The slag (Figure 3a) was acquired from the Siderurgia Nacional company, Portugal, with an extensive particle size distribution. A three-step mechanical activation process was followed. In the first step, the slag was crushed using a Los Angeles abrasion testing machine, then using a jaw crusher and finally a ball mill. The resulting material (Figure 3b) showed an average particle size of ~25 μm. The chemical characterization of the slag, obtained using X-ray fluorescence (XRF), is presented in Table 2.

Table 2: X-ray fluorescence results of EAFS and FA

Material	CaO (%)	SiO_2 (%)	Al_2O_3 (%)	Fe_2O_3 (%)	MgO (%)	SO_3 (%)	Na_2O (%)	K_2O (%)	LOI (%)
EAFS	25.5	16.0	9.16	25.7	5.12	0.3	0.17	0.03	9.63
FA	3.6	57.8	20.9	7.4	1.0	0.6	1.0	1.7	3.8

Figure 3: EAFS as-received (a- left) and after milling to the required size for use as a precursor in concrete (b-right)

- Fly ash:

FA was acquired from a coal power plant in Sines, Portugal. The as-received FA had an average particle size of ~15 μm. The chemical composition of the FA is shown in Table 2.

- Alkaline solution:

To prepare the alkaline solution, pure NaOH pellets (99% purity) were acquired from a local supplier in Lisbon. A commercial superplasticizer (SP) that consists of a β-naphthalene sulfonic acid formaldehyde condensate was added to the alkaline solution before mixing. Tap water was used as solvent.

- Aggregates:

Five grades of natural aggregates were procured from different local sources. Two sizes of natural silica sand were used as fine aggregates and three sizes of crushed limestone were used as coarse aggregates. The particle size ranges, proportions and the water absorption of are summarized in Table 3. The particle size distribution of the aggregates comply with the requirements of ASTM C33 [44].

Table 3: Characterization of the aggregates used in the concrete mixes

Aggregates	Nominal size	Oven-dried density	Water absorption	Mass ratio	General size
	mm	(kg/m^3)	%	%	
Fine sand	0/1	2637	0.4	30	Fine aggregates
Coarse sand	0/4	2617	0.5	70	
Rice grain gravel	2/5.6	2600	1	15	Coarse aggregates
Fine gravel	5.6/11.2	2600	1.2	25	
Coarse gravel	10/20	2600	1.4	60	

2.2 Concrete mix design

An experimental program was developed for the mixes shown in Table 4. Mixes 1-3 consist of precursors of 100% FA as a reference AAC because they are established in the literature, while mixes 7-9 are based on 100% EAFS precursors. To gain the co-benefits, mixes 4-6 were produced with proportions of 50% FA and 50% EAFS as precursors. Based on data from the literature, it was decided that synthesizing alkaline solution with a concentration of 10% Na_2O to binder would yield the optimum concrete performance. The literature also suggests that the optimum activator for slag would be a SiO_2/Na_2O ratio close to 2. However, it was decided not to include SS in the mix to maintain a low level of economic and environmental impacts. The water to precursor ratio varies between 0.30, 0.40 and 0.50 and the content of SP varied according to the results of trial mixes to target a S3/S4 slump class.

Table 4: Mix design of mixes 1-9

Components	Mass of each component per AAC mix (kg/m³)								
	M1	M2	M3	M4	M5	M6	M7	M8	M9
FA	299	292	284	150	146	142	0	0	0
EAFS	0	0	0	167	163	158	334	325	316
SP	4	1	0	5	1	0	5	3	2
Water	104	131	155	104	131	155	104	130	155
NaOH	39	38	37	41	40	39	43	42	41
Fine sand 0/1	265	258	251	265	258	251	264	257	250
Coarse sand 0/4	613	597	581	613	597	581	612	595	579
Sand-Gravel 2/5.6	174	169	165	174	169	165	174	169	164
Fine gravel 5.6/11.2	290	282	275	290	282	275	290	282	274
Coarse gravel 10/20	696	678	660	696	678	659	695	676	658
	Mix design ratios								
Effective water/ precursor	0.3	0.4	0.5	0.3	0.4	0.5	0.3	0.4	0.5
SP/ precursor (%)	1.5	0.5	0	1.5	0.5	0	1.5	1	0.5
FA/ precursor (%)		100			50			0	
EAFS/ precursor (%)		0			50			100	
Na_2O/ precursor (%)					10				

2.3 Concrete mixing, casting and curing procedures

The alkaline solution was prepared by dissolving the SH pellets in water gradually and then left to cool down for 24 hours. On the mixing day, the solution was added first in the mixer along with the SP and the precursor and then mixed for 5 minutes. After that, the mixer was stopped until the aggregates were added and then all the components were mixed together for

another 5 minutes. After the slump test was carried out, the moulds were sprayed with paraffin and concrete was cast inside and vibrated according to EN 12390-2 [45]. After casting, the specimens were wrapped with thin plastic film for sealing, and then placed in a thermal curing chamber. Specimens were cured for the first 24 hours in an oven at 70 °C. Afterwards, the specimens were demoulded and left to cure in a chamber with a temperature of 23 ± 2 ºC and a relative humidity of 100% until testing day.

2.4 Hardened concrete test methods

- Slump:

The slump test was performed on each fresh mix according to the EN 12350-2 standard [50]. Mixes with a slump <100 mm were rejected and the SP was adjusted accordingly.

- Compressive strength:

After 28 days of curing, 150 mm cubic samples were tested for compressive strength according to the EN 12390-3 standard [50] using a TONI PACT 3000 universal testing machine with a 12 kN/s loading rate.

- Chloride ion penetration:

After 28 days of curing, three cylindrical specimens of 100 mm in diameter and 50 mm in thickness per concrete mix were cut from the cast cylinders. As per the BUILD NT 492 standard [47], the specimens were placed in a clean and dry desiccator and air vacuumed for 3 hours. After that, the samples were vacuumed in a lime solution for 1 hour then left for 20 more hours to saturate in the lime solution. On testing day, the specimens were placed in sealed rubber forms and then in the rapid chloride ion penetration testing (RCPT) apparatus. The chloride diffusion coefficient of each specimen D_{nssm} was then calculated using the equation from the standard.

- Carbonation:

After 21 days of curing, six cylindrical specimens of 100 mm diameter and 30 mm thickness were cut from the originally cast samples of each mix following the LNEC E391 standard [48]. At 28 days, two specimens of each mix were placed in a carbonation chamber with a CO_2 concentration of 5 ±0.1%, temperature of 23 ±3 °C and relative humidity of 60 ±5% for 14 days.

After the exposure period ended, the samples were broken into four pieces and sprayed with phenolphthalein. The depth of carbonation was then measured using a Vernier calliper across each face of the broken fraction of each sample and averages were recorded for every mix.

2.5 Applying the ECO_2 framework

2.5.1 Scope and scenarios

ECO_2 framework is applied in 10 steps as in Figure 4, are divided between two stages.

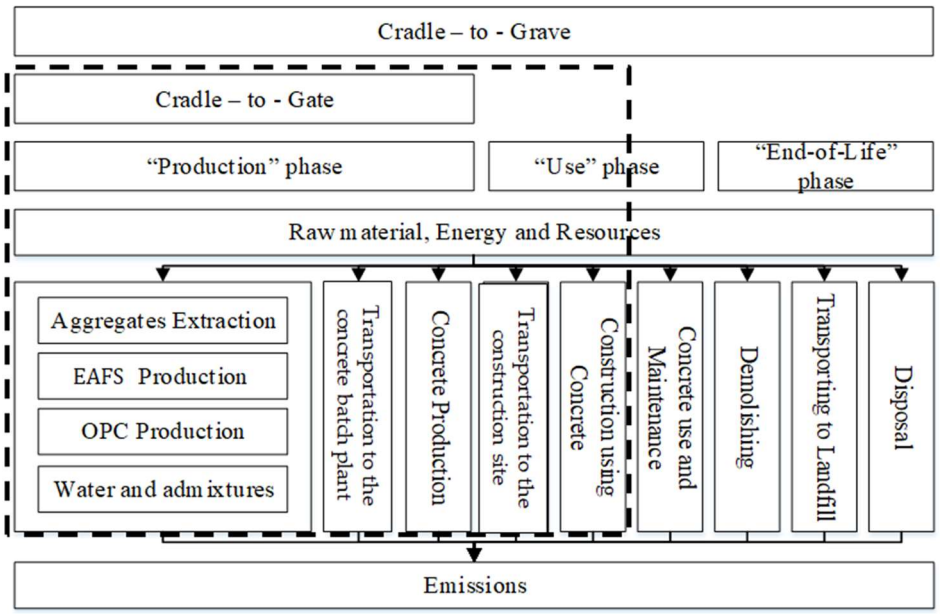

Figure 4: Typical LCA boundary and the scope selected for this study

The first stage includes: defining the scope and the scenarios; defining the alternative, and collecting the necessary inventory data. After that, the second stage includes calculating the functional unit for each alternative, assessing the environmental and economic impact and finally the ECO_2 index is evaluated in an attempt to optimize the alternatives. In a typical LCA study, the scope for a concrete product life cycle could be Cradle-to-Gate, which means including all processes and emissions until the production of its different constituents or Cradle-to-Grave, which includes the "Use" and "End-of-Life" phases. In this study, as in Figure 4, it was decided to have a Cradle-to-Gate scope, due to the similarity in the remaining processes across all alternatives.

To account for uncertainty as per the LCA recommendations, two scenarios were defined: a reinforced concrete scenario (S1) and a plain/mass concrete scenario (S2). The former would

account for the durability of concrete alternatives under study, while the latter would assume the AAC fulfils the service life requirements. Since Eurocode 2 specifies a minimum of 10 MPa for the characteristic compressive strength of cubic specimens, this value was set as the required compressive strength (threshold value) of both concrete scenarios. Preliminary testing showed very low strength values obtained from testing mixes 7, 8 and 9, they would not fulfil the basic project requirements and, hence, are excluded from the comparison. The comparison between the remaining six alternatives (M1-M6) was based on a unit volume of concrete that has a minimum slump of 100 mm and a targeted service life of 50 years.

2.5.2 Definition of alternatives

The next step would be to enter the mixing proportions of each mix (conventional and non-conventional/alternative mixes) per cubic meter as per the mix design in Table 4. This would then serve as the basis for quantifying the environmental and economic impact of each alternative as per the ECO_2 logic.

2.5.3 Environmental inventory data

- Raw materials production

The only primary production data collected for this study is the energy required for EAFS processing. For every 20 kg, the LA abrasion testing machine was used for 2 hours, then the jaw-crushing machine was used for 1 hour and finally the ball-milling machine was used for 2 hours. The power input for each of these machines is 800 W, 500 W and 1200 W, respectively. Hence, the energy demand allocated for the production of each kg of EAFS is calculated as follows. Slag processing energy = (2 h × 0.8 kW + 1 h × 0.5 kW + 2 h × 1.2 kW) / 20 kg = 83 kWh/tonne. This is translated to the environmental indicators by multiplying it by the average impact per unit energy of the Portuguese energy grid. The inventory data concerning the unit energy and the data concerning the production of the remaining concrete constituents are averages from a secondary database that was published in a systematic literature review [49], as seen in Table 5.

- Raw materials transportation

All materials were produced in Portugal and transported locally, using a small truck. An extra 70% of the impact is added to account for the return ride. The transportation distances are summarized in Table 5.

- Concrete construction

The energy and emissions involved in the concrete construction phase are the combination of that resulting from mixing, transporting to site, casting and curing. The curing method followed for all AAC mixes within the scope of this experimental campaign included 24 hours in the thermal curing chamber. The chamber, operating at 70 ºC, used a heating unit with an input power equal to 2000 W. The oven has a capacity of approximately 25 cubes (150 mm), which means that the energy required for curing could be calculated as: concrete curing energy = 2 kW × 24 h / (25 cubes × 0.15 m × 0.15 m × 0.15 m) = 20 kWh/m^3. The energy required for the mixing and placing concrete was assumed as 20 kWh/m^3 and the distance from the batch plant to the site as 80 km. The aforementioned data was estimated based on the secondary database in [49].

2.5.4 Economic inventory data

The economic impact of the production of a concrete mix is basically the sum of the costs of the production and transportation of all its constituents. However, similarly to the ecological impact calculations, in order to account for the whole life cycle of concrete, the economic impact for every concrete mix needs to also include that of the transportation of concrete to the construction site as well as the processes of construction and demolition.

The primary data provided by the suppliers for the purchasing prices of all constituents of the AAC studied was added to the ECO_2. The cost of transporting the raw materials to the concrete batch plant was calculated based on an average unit price for transportation from the database in [45]. It is important to note that, unlike the environmental impact calculations, the return distance was not accounted for because it is assumed as included in the price. The summary of the data is found in Table 5.

Table 5: Summary of the environmental and economic inventory data for the LCA study

		Market price per unit	Distance	GWP	ODP	AP	EP	ADPE	POCP	CED	FW
		€ per unit	km	kg·co^{2}	kg·cfc^{-11}	kg·so^{2}	kg·po^{4}	kg·sb$_{eq}$	kg·c2H$_{4eq}$	MJ	m^{3}
Electricity from coal (/kWh)		-	-	3.19E-01	7.70E-10	1.83E-03	2.96E-04	2.60E-03	7.09E-05	9.10E-04	3.75E+00
Portuguese unit energy impact (/kWh)		0.11	-	3.75E-02	1.59E-09	0.00E+00	1.08E-04	2.79E-04	6.65E-06	8.30E-01	2.93E-01
Impact per distance (/km) Small truck (< 25 tonnes)		0.05	-	2.90E-01	1.90E-07	7.60E-05	1.67E-04	8.14E-04	6.11E-05	3.15E+00	3.62E-01
Binder (/kg)	EAFS	0	30	3.11E-03	1.32E-10	0.00E+00	9.00E-06	2.31E-05	5.52E-07	6.89E-02	2.43E-02
	Fly ash (0.3% allocation)	0.036		9.56E-03	2.31E-11	5.48E-05	8.88E-06	7.79E-05	2.13E-06	2.73E-05	1.13E-01
Aggregates (/kg)	Natural coarse	0.01	15	1.03E-02	1.05E-09	1.53E-05	5.39E-06	1.49E-05	4.53E-06	7.19E-02	2.90E-02
	Natural fine	0.01		6.72E-03	4.75E-08	8.10E-06	2.82E-06	5.07E-05	9.83E-07	5.78E-02	2.11E-02
Chemical admixtures - Superplasticizer (/kg)		1.4	20	9.08E-01	1.09E-07	5.44E-02	9.24E-04	4.94E-03	1.88E-04	1.98E+01	6.98E-01
Activator (/kg)	SH	0.51	100	1.27E+00	1.14E-07	2.93E-03	6.63E-04	9.30E-03	2.61E-04	6.35E+00	2.24E+00
	Water	0.277	0	2.50E-04	5.57E-12	0.00E+00	1.26E-07	6.83E-07	6.32E-08	2.95E-04	1.06E-03

ADP - Abiotic depletion potential; AP - Acidification potential; EP - Eutrophication potential; GWP - Global warming potential; POCP - Photochemical ozone creation potential; CD - Cumulative energy demand; FW - Fresh water use

2.5.5 Functional Unit calculations

The functional unit (FU) is a key element in a LCA and is responsible for the quantification of the environmental and economic impact indicators [49]. In most sustainability frameworks, the functional unit is assumed as simply a unit volume of concrete (1 m^3). However, calculating the FU according to the ECO_2 framework is done in two stages. The first is checking whether the minimum requirements of the project, which are workability and strength, are met. For every alternative (*i*), the user inputs the values for slump (Yslump) and strength (Ystrength) and if Yslump (*i*) < Yslump (required) or Ystrength (*i*) < Y strength (required), the alternative is rejected. Note that, as explained in the scenario definition, the required slump and strength for this case study are 100mm and 10 MPa respectively. If an alternative achieves the minimum requirement, the functional unit is defined as per the following equation 1, where N is the replacement ratio of the concrete alternative, reflecting the number of times it would need to be replaced to fulfil the required service life. If the concrete alternative is plain concrete, which is the case in scenario 1, it is assumed as durable enough to sustain itself throughout the required service life without need for maintenance or replacement. Hence, in scenario 1, for all 6 alternatives, N is equals to 1 and FU is equals to 1 m^3 of concrete.

$$FU_i = N_i * 1m^3 \quad (1)$$

For each reinforced concrete alternative in scenario 2, N is calculated as per equation 2 where SL_R is the required service life, which is 50 years in this case. $SL_{P\text{-}Cl}$ and $SL_{P\text{-}Cr}$ are the predicted service life for this alternative against chloride-induced corrosion and carbonation-induced corrosion respectively.

$$N = \frac{SL_R}{\min\left(SL_{P-Cl}, SL_{P-Cr}\right)} \quad (2)$$

The main durability parameters of concrete are the resistance to chloride penetration and carbonation [49]. Hence, these are the ones considered within the ECO_2 framework to predict the service life of concrete. Service life predictions against chloride-induced corrosion are defined in standards as the duration that the chloride content at the surface of the steel reinforcement takes to reach the chloride threshold [46]. The model, developed based on Fick's 2nd law of diffusion, predicts the service life $SL_{p\text{-}cl}$ as per equations 3 and 4 at the time when C(x, t) is equal to C_{cr}:

$$C(x,t) = C_o * erfc(\frac{x}{2*\sqrt{D_t * t}}) \quad (3)$$

$$D_t = D(\frac{t_o}{t})^{\propto} \quad (4)$$

Where, D is the chloride diffusion coefficient (m^2/s), C_{cr} the chloride threshold level (%), C_o the chloride concentration on the concrete surface estimated at 1 %, X the concrete cover assumed as 70 mm in this case study, α an aging factor, and t the service life expected for the durability against chloride penetration $SL_{R\text{-}Cl}$, in years.

$$SL_{P-Cr} = \left(\frac{X}{K_n}\right)^2 \quad (5)$$

$$K_n = K_a\sqrt{\frac{CC_n}{CC_a}} \quad (6)$$

The durability of a concrete alternative against carbonation is a measure of the time at which the depth of carbonated concrete (X_c) is equal to the concrete cover (X). Hence, the model used to predict the service life of concrete alternatives depends on K_n, which is the natural carbonation rate of concrete, to calculated $SL_{p\text{-}Cr}$ as seen in equation 5. *I*n cases such as this study where an accelerated carbonation test is performed, K_n is correlated to the accelerated carbonation rate K_a using equation 6. The values for CC_n, which is the CO_2 % concentration in the environment and CC_a, which is that in the carbonation chamber in which the test was done are 0.05% and 5% respectively.

2.5.6 Ecological impact calculations

The first step is to calculate the impact of producing concrete per unit volume is by multiplying the impact of producing and transporting every constituent by its mixing proportion for every alternative. The second step is to add the impact from concrete construction as per equation 7. The environmental impact is demonstrated through eight mid-point indicators: Global Warming Potential (GWP), Ozone Depletion Potential (ODP), Acidification Potential (AP), Eutrophication Potential (EP), Abiotic Depletion Potential (ADPE), photochemical ozone creation potential (POCP), Cumulative Energy Demand (CED) and Fresh Water (FW).

$$\frac{GWP_i}{m^3} = \sum_{j=1}^{n}(\frac{GWP_j\, upstream}{kg} * \frac{kg_j}{m^3}) + \frac{GWP_i\, construction}{m^3} \quad (7)$$

The total impact per unit volume is then multiplied by the functional unit of each alternative. Once the total impact per functional unit is calculated for each alternative, it is then

normalized, according to equation 8, with the alternative with the lowest impact in each indicator getting a value of 1 and the one with the highest impact a value of 0. Finally, the single environmental indicator, which is called the ecological indicator within to the ECO_2 algorithm, is calculated based on the weighted average of all eight indicators.

$$V_i' = \frac{max\,(V_i) - V_i}{max\,(V_i) - min\,(V_i)} \quad (8)$$

2.5.7 ECO_2 index calculations

After calculating the single ecological indicator for each alternative, the single economic indicator is calculated as such. Using the economic inventory data, the per unit volume total cost of each alternative is calculated by summing up the cost of production and construction. After that, the single economic indicator Z is calculated as the FU of each alternative multiplied by the total cost per unit volume.

The single economic indicator Z is then normalized using the same equation 8 with the cheapest alternative getting a score of 1 and the most expensive as 0. The ECO_2 index is then calculated for each alternative as an average of the scores of its normalized single ecological index V and the economic one Z as per equation 9.

$$ECO_{2_i} = V_i * 0.5 + Z_i * 0.5 \quad (9)$$

3. Results and discussion

3.1 Functional unit results

For the 6 mixes that were fulfilling of the minimum requirements (slump > 100 mm and strength > 10 MPa), the results of the experimental work show the following. First, as expected, the higher the water to precursor ratio, the higher the workability of the mix. However, the slump results show no clear correlation between the changes of the precursor from FA to EAFS. The 28-day compressive strength results show that replacing FA with EAFS as a precursor in the AAC resulted in a decrease in strength, mostly due to the lower amount of amorphous silica phases in the latter. In addition, in the 100% FA mixes (M1-3), the higher the water/precursor ratio, the lower the strength.

As seen in Figure 5, mixes with 50% EAFS as a precursor (mixes 4-6) have around 50% lower chloride diffusion coefficient. The enhanced resistance to chloride penetration could be attributed to the denser microstructure of the EAFS based binder from the literature [36]. This resulted in longer expected service life for these mixes (180 years) compared to that of the 100% FA mixes (100 years).

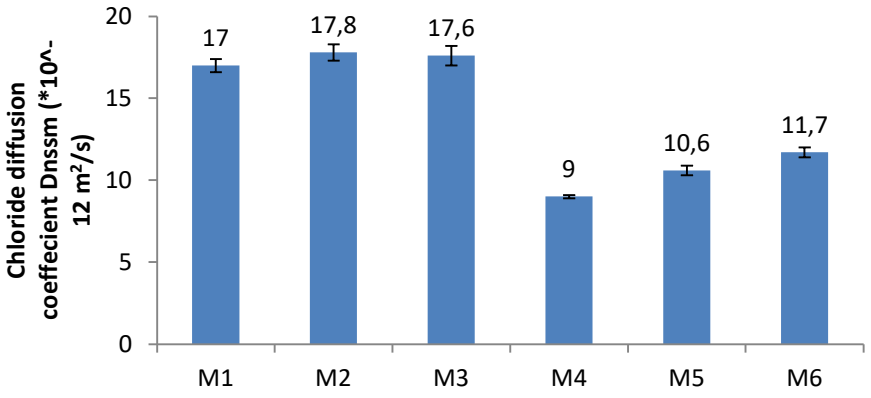

Figure 5: Chloride diffusion rates of the AAC mixes tested

As seen in Figure 6, the results of this experiment show that the higher the water/precursor ratio, the higher the carbonation rate. The same applies for replacing FA with EAFS as a precursor, i.e. the higher the replacement ratio, the lower the resistance to carbonation of the AAC mix is. Hence, the expected service life against carbonation for the 50% EAFS mixes (4-6) was around 50% lower than that of mixes 1-3 as seen in Table 6. As a result, the functional unit for mixes 1-3 was 1.3, 1.4 and 1.5 respectively, while that of mixes 4-6 was 1.8, 1.9 and 2 respectively, which affects the impact assessment linearly.

Table 6: A summary of the experimental results and functional unit calculations of mixes 1-6

Alternative number		1	2	3	4	5	6
1. Slump	mm	105	200	180	110	190	170
2. 28-day compressive strength	MPa	24	19	14	12	11	10
3. 28-day diffusion coefficient (D_{nssm})	*10^-12 m²/s	17	17.8	17.6	9	10.6	11.7
4. Accelerated carbonation rate	mm/√year	82	85	88	94	97	100
5. Natural carbonation rate	mm/√year	8.2	8.5	8.8	9.4	9.7	10
Predicted service life as per chloride penetration	Years	100	100	100	180	170	160
Predicted service life as per carbonation	Years	37	35	32	28	27	25
Replacement ratio (N)	-	1.3	1.4	1.5	1.8	1.9	2.0
Functional unit	m³	1.3	1.4	1.5	1.8	1.9	2.0

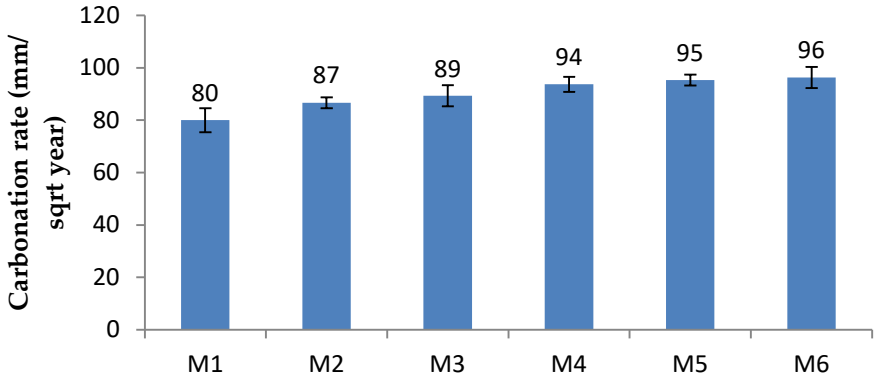

Figure 6: Accelerated carbonation rate of the AAC mixes tested

3.2 Impact assessment

3.2.1 Ecological impact assessment

- Scenario 1 (plain concrete):

All mixes are assumed to fulfil the service life requirements and hence have an equal FU of 1. As seen in Figure 7, the contribution of the transportation impact to the total impact of each constituent of the AAC mixes was minimal. Therefore, the comparison between alternatives is purely dependant on the environmental impact of the concrete constituent's production impact.

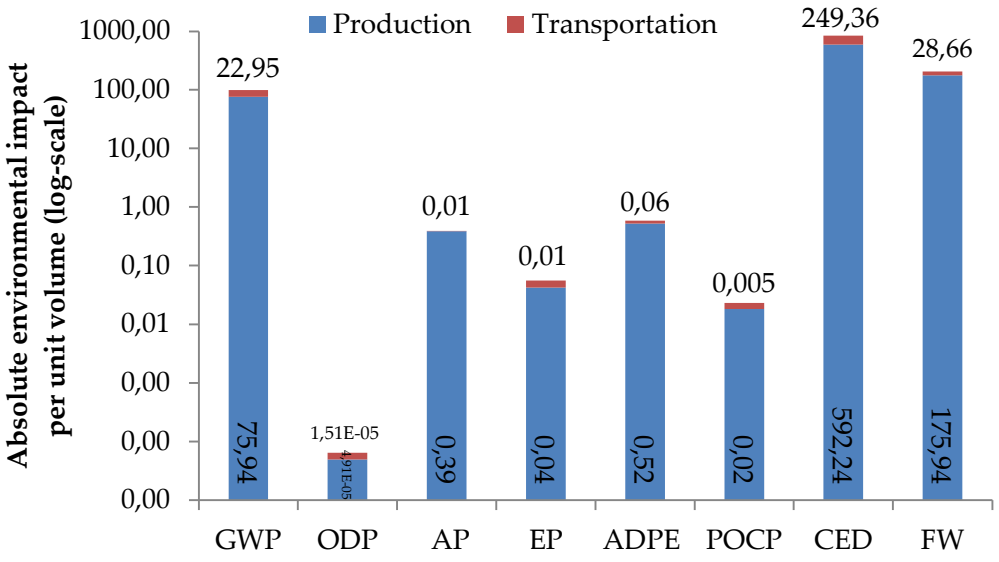

Figure 7: Contribution of transportation processes to the total environmental impact of alternative 1

Due to the higher impact of SP, SH and FA compared to water and EAFS, increasing the W/P ratio and replacing FA with EAFS as precursors yields a binder with a better (lower) environmental impact. As seen in Figure 8, mixes 4-6 with 20% EAFS showed 60-70% better

(lower) environmental impact scores on average compared to mixes 1-3 with 100% FA. The same is observed for mixes 3 and 6 with a W/P of 0.5 compared to mixes 1 and 4, respectively.

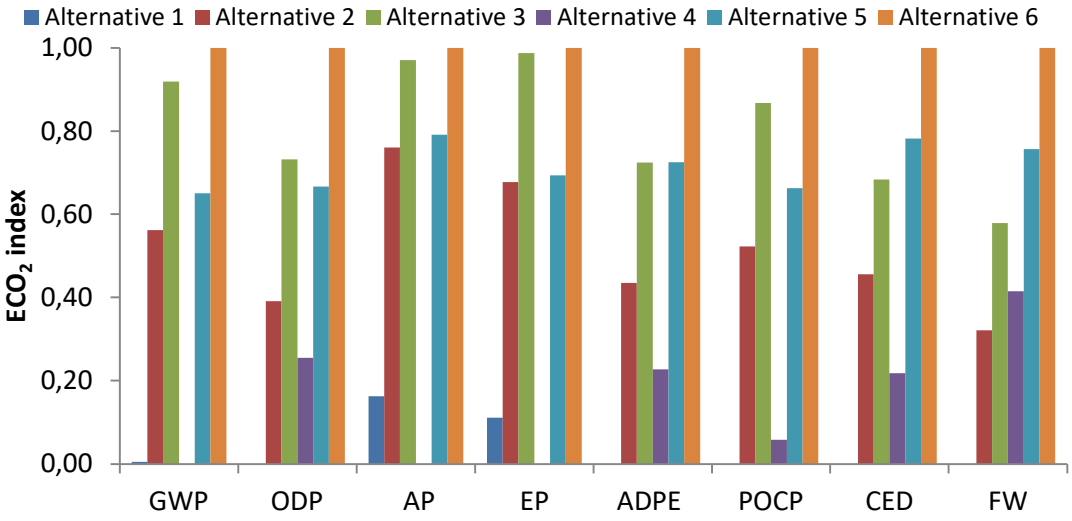

Figure 8: Normalized environmental impact indicators for plain concrete scenario

- Scenario 2 (reinforced concrete):

Due to the lower carbonation resistance of the mixes with EAFS, mixes 4-6 were calculated to have a functional unit of 1.8, 1.9 and 2 respectively in the 50 years reinforced concrete scenario as opposed to 1.3, 1.4 and 1.5 for mixes 1-3. Hence, the environmental impact of the EAFS was almost doubled which overcame the advantage observed in the plain concrete scenario as seen in the normalized environmental impact scores in Figure 9.

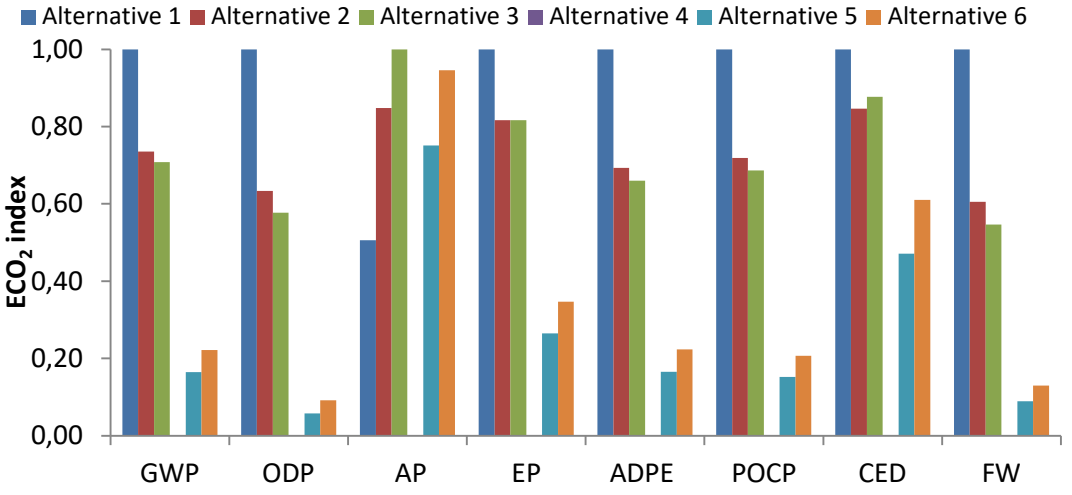

Figure 9: Normalized environmental impact indicators for plain concrete scenario

3.2.2 Calculation of the ECO_2 index

- Scenario 1 (plain concrete):

As seen in Table 5, the constituents with the highest environmental impact, FA, NaOH and the superplasticizers, also happen to have the highest cost. Hence, as seen in Figure 10, mixes with higher W/P ratios (mix 3 compared to 1 and mix 6 compared to 4) and 50% replacement of FA with EAFS (mixes 4-6 compared with mixes 1-3) scored a higher (cheaper) single economic impact indicator. Since this is aligned with the single ecological score comparison, the ECO_2 score followed the same trend.

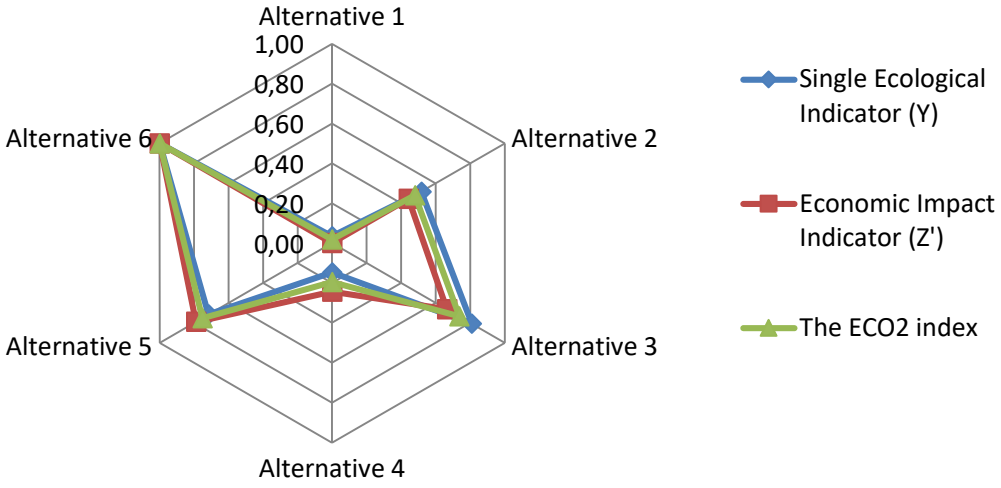

Figure 10: Single Ecological, Economic and ECO_2 score comparison in scenario 1

- Scenario 2 (reinforced concrete):

In the reinforced concrete scenario, mixes 1, 2 and 3 with 100% FA appear to have a far superior sustainability score as seen in Figure 11 because the advantage in the economic and environmental impact for mixes 4-6 was offset by the major disadvantage in terms of the functional unit. The reason is that, following the literature recommendations, the optimum activators for slag-based precursors require a SiO_2/Na_2O ratio between 1 and 2. However, this would have meant adding SS and increasing the environmental and economic impact. Both of these observations are consistent with the hypothesis provided in Table 1.

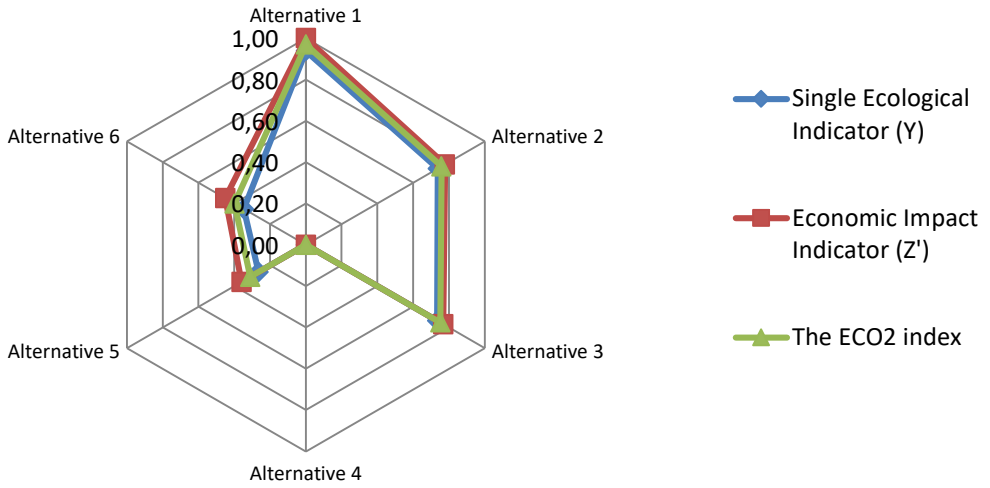

Figure 11: Single Ecological, Economic and ECO_2 score comparison in scenario 2

3.3 Discussion of the results

3.3.1 Contextualizing absolute impact

Besides the local comparison between the alternatives, a comparison was made in Table 7 against values of global thresholds from Kurda et al. [51] for selected indicators: GWP, CED and basic cost per cubic meter. Accordingly, all six mixes in this case study appear to have "very low" global warming potential and cumulative energy demand. The costs of all mixes are also "low" except for mix 1 and mix 4 which are normal.

Table 7: Comparison between the GWP, CED and cost of the studied alternatives against global thresholds

Scenario	Global warming potential kg co_2/m^3	Energy consumption MJ/m^3	Total cost €/m^3
Alternative 1	87.71	841.61	73.4
Alternative 2	81.11	761.47	67.7
Alternative 3	76.80	721.49	64.9
Alternative 4	85.29	803.23	70.3
Alternative 5	77.59	704.13	63.3
Alternative 6	73.23	665.84	60.6
Very High	> 522	> 3388	> 82
High	392-522	2541-3388	75-82
Normal	354-392	2299-2541	69-75
Low	224-354	1452-2541	62-69
Very Low	< 224	< 1452	< 62

3.3.2 Sensitivity analysis

In order to account for the uncertainty of the data, it is recommended to perform a sensitivity analysis on the most significant input variables of the study. In this study, there were two main variables in the mix design, the W/P ratio and the % replacement of FA with

EAFS as a precursor. Hence, a sensitivity analysis was designed to calculate the effect of changing the transportation distance and market price of the FA and slag on the resulting ECO_2 index score. Varying each of the three chosen variables by ±50% resulted in minimal (1-2%) impact on the ECO_2 index score of the studied variables, which shows that the results and conclusions are consolidated.

4. Conclusions

This paper analyses the sustainability of a promising concrete alternative, namely EAFS-based AAC. Preliminary investigation of the available literature showed that there are few studies on the performance of the material and none on its environmental and economic impacts. Hence, this paper targeted the assessment of several EAFS AAC alternatives through a concrete sustainability assessment framework previously suggested by the authors; the ECO_2 framework.

Several AAC mixes were designed to test the effect of changing the precursor from FA to EAFS and changing the water: precursor ratio on three sustainability pillars: technical performance, environmental and economic impact. The tests performed on the AAC mixes were slump, compressive strength, chloride penetration and carbonation. After that, data from the test results as well as the site-specific environmental and economic properties was collected and the sustainability of the alternatives were compared according to the ECO_2 framework.

The preliminary conclusion was that, due to the deteriorated functional properties of the EAFS-based AAC mixes, the optimum mixes were those with FA only. However, this was only valid in terms of reinforced concrete, because when a scenario with plain concrete was assumed, the EAFS-based mixes exhibited a significantly improved sustainability potential using the ECO_2 index. This could be primarily attributed to the low cost and environmental impact (almost negligible) of the EAFS. In both cases, the original hypothesis concerning the effect of W/P ratio was proven and the results from both scenarios were run against the sensitivity of some input data and showed minimal effect.

Due to the complexity of the sustainability assessment calculations, it would not have been easy for users to analyse the optimum mix based on the combined functional, environmental and economic impacts. Hence, the use of the ECO_2 framework was critical to make this

assessment easier and allow for the optimization of the mixing proportions of AAC mixes with a target of the highest achievable single sustainability score.

Acknowledgments

The authors gratefully acknowledge the support of the Portuguese Foundation for Science and Technology (Fundação para a Ciência e Tecnologia) through the research project PTDC/ECI-CON/29196/2017 (RInoPolyCrete) and CERIS Research Institute, Instituto Superior Técnico, Universidade de Lisboa.

References

1. Monteiro, P.J., Miller, S.A. and Horvath, A., 2017. Towards sustainable concrete. *Nature materials*, *16*(7), pp.698-699. https://doi.org/ 10.1038/nmat4930
2. Serres, N., Braymand, S. & Feugeas, F. 2016. Environmental evaluation of concrete made from recycled concrete aggregate implementing life cycle assessment. *Journal of Building Engineering,* 5**,** 24-33. https://doi.org/10.1016/j.jobe.2015.11.004
3. Colangelo, F., Forcina, A., Farina, I. and Petrillo, A., 2018. Life cycle assessment (LCA) of different kinds of concrete containing waste for sustainable construction. *Buildings, 8*(5), 70. https://doi.org/10.3390/buildings8050070
4. Habert, G., D'espinose De Lacaillerie, J. B. & Roussel, N. 2011. An environmental evaluation of geopolymer based concrete production: reviewing current research trends. *Journal of Cleaner Production,* 19**,** 1229-1238. https://doi.org/10.1016/j.jclepro.2011.03.012
5. Ashby, M. F. 2012. Materials and the environment: Eco-informed material choice, *Elsevier Science*.Ch 10.
6. Miller, S. A., Monteiro, P. J. M., Ostertag, C. P. & Horvath, A. 2016. Concrete mixture proportioning for desired strength and reduced global warming potential. *Construction and Building Materials,*128**,** 410-421. https://doi.org/10.1016/j.conbuildmat.2016.10.081
7. Yuli, S., Guan, D., Zheng, H., Ou, J., Li, Y., Meng, J., Mi, Z., Liu, Z. and Zhang, Q., 2018. China CO_2 emission accounts 1997-2015. *Scientific data*, *5*, 170-201. https://doi.org/ 10.1038/sdata.2017.201
8. Miller, S.A., John, V.M., Pacca, S.A. and Horvath, A., 2018. Carbon dioxide reduction potential in the global cement industry by 2050. *Cement and concrete research*, 114,115-124. https://doi.org/10.1016/j.cemconres.2017.08.026
9. Puertas, F., Palacios, M., Manzano, H., Dolado, J.S., Rico, A., Rodríguez, J. 2011. A model for the C-A-S-H gel formed in alkali-activated slag cements. *Journal of the European Ceramic Society*, 31 (12), 2043-2056. https://doi.org/10.1016/j.jeurceramsoc.2011.04.036
10. Nasir, M., Al-Amoudi, O.S.B. and Maslehuddin, M., 2017. Effect of placement temperature and curing method on plastic shrinkage of plain and pozzolanic cement

concretes under hot weather. *Construction and Building Materials*, *152*, pp.943-953. https://doi.org/10.1016/j.conbuildmat.2017.07.068
11. Navarro, R., Zornoza, E., Garcés, P., Sánchez, I. and Alcocel, E.G., 2017. Optimization of the alkali activation conditions of ground granulated SiMn slag. *Construction and Building Materials*, *150*, pp.781-791. https://doi.org/10.1016/j.conbuildmat.2017.06.064
12. Provis, J.L., Arbi, K., Bernal, S.A., Bondar, D., Buchwald, A., Castel, A., Chithiraputhiran, S., Cyr, M., Dehghan, A., Dombrowski-Daube, K. and Dubey, A., 2019. RILEM TC 247-DTA round robin test: mix design and reproducibility of compressive strength of alkali-activated concretes. *Materials and Structures*, *52*(5), 99. https://doi.org/10.1617/s11527-019-1396-z
13. Lothenbach, B., Scrivener, K. and Hooton, R.D., 2011. Supplementary cementitious materials. *Cement and concrete research*, *41*(12), pp.1244-1256. https://doi.org/10.1016/j.cemconres.2010.12.001.
14. Puertas, F., Martínez-Ramírez, S., Alonso, S. and Vazquez, T., 2000. Alkali-activated fly ash/slag cements: strength behaviour and hydration products. *Cement and Concrete Research*, *30*(10),.1625-1632. https://doi.org/10.1016/S0008-8846(00)00298-2
15. Rashad, A.M., 2019. A synopsis of carbonation of alkali-activated materials. *Green Materials*, *7*(3), 118-136. https://doi.org/10.1680/jgrma.18.00052
16. Kumar, R., Kumar, S. and Mehrotra, S. P. 2007. Towards sustainable solutions for fly ash through mechanical activation. *Resources, Conservation and Recycling*, 52(2), 157-179. https://doi.org/10.1016/j.resconrec.2007.06.007
17. Duxson, P., Provis, J. L., Lukey, G. C., Mallicoat, S. W., Kriven, W. M. and Van Deventer, J. S. J., 2005. Understanding the relationship between geopolymer composition, microstructure and mechanical properties, *Colloids and Surfaces A: Physicochemical and Engineering Aspects*, 269(1-3), 47-58. https://doi.org/10.1016/j.colsurfa.2005.06.060.
18. Ravikumar, D. & Neithalath, N. 2013. Electrically induced chloride ion transport in alkali activated slag concretes and the influence of microstructure. *Cement and Concrete Research*, 47, 31-42. https://doi.org/10.1016/j.cemconres.2013.01.007.
19. Bernal, S., San Nicolas, R., Provis, J., Mejía De Gutiérrez, R. & Van Deventer, J. 2014. Natural carbonation of aged alkali-activated slag concretes. *Materials and Structures*, 47, 693-707. https://doi.org/10.1617/s11527-013-0089-2.
20. Nasir, M., Johari, M.A.M., Yusuf, M.O., Maslehuddin, M. and Al-Harthi, M.A., 2019. Synthesis of alkali-activated binary blended silico-manganese fume and ground blast furnace slag mortar. *Journal of Advanced Concrete Technology*, *17*(12), pp.728-735. https://doi.org/10.3151/jact.17.728. https://doi.org/10.3151/jact.17.728.
21. Nasir, M., Johari, M.A.M., Yusuf, M.O., Maslehuddin, M., Al-Harthi, M.A. and Dafalla, H., 2019. Impact of slag content and curing methods on the strength of alkaline-activated silico-manganese fume/blast furnace slag mortars. *Arabian Journal for Science and Engineering*, *44*(10), pp.8325-8335. https://doi.org/10.1007/s13369-019-04063-7
22. Nasir, M., Johari, M.A.M., Maslehuddin, M., Yusuf, M.O. and Al-Harthi, M.A., 2020. Influence of heat curing period and temperature on the strength of silico-manganese fume-blast furnace slag-based alkali-activated mortar. *Construction and Building Materials*, *251*, p.118961. https://doi.org/10.1016/j.conbuildmat.2020.118961.
23. Jiang, M., Chen, X., Rajabipour, F. and Hendrickson, C.T., 2014. Comparative life cycle assessment of conventional, glass powder, and alkali-activated slag concrete and mortar. *Journal of Infrastructure Systems*, *20*(4), 401-420. https://doi.org/10.1061/(ASCE)IS.1943-555X.0000211

24. Provis, J.L., 2014. Geopolymers and other alkali activated materials: why, how, and what?. *Materials and structures*, *47*(1-2), 11-25. https://doi.org/10.1617/s11527-013-0211-5
25. Garcia-Lodeiro, I., Fernández-Jimenez, A., Pena, P. and Palomo, A., 2014. Alkaline activation of synthetic aluminosilicate glass. *Ceramics International*, *40*(4), 5547-5558. https://doi.org/10.1016/j.ceramint.2013.10.146
26. Komljenovi, M., Baarevi, Z., Marjanovi, N. and Nikoli, V. (2013). External sulfate attack on alkali-activated slag. *Construction and Building Materials*, 49, 31-39. https://doi.org/10.1016/j.conbuildmat.2013.08.013
27. Passuello, A., Rodríguez, E. D., Hirt, E., Longhi, M., Bernal, S. A., Provis, J. L. & Kirchheim, A. P. 2017. Evaluation of the potential improvement in the environmental footprint of geopolymers using waste-derived activators. *Journal of Cleaner Production*, 166, 680-689. https://doi.org/10.1016/j.jclepro.2017.08.007
28. Jiang, Y., Ling, T.C., Shi, C. and Pan, S.Y., 2018. Characteristics of steel slags and their use in cement and concrete—A review. *Resources, Conservation and Recycling*, *136*, 187-197. https://doi.org/10.1016/j.resconrec.2018.04.023
29. Bignozzi, M.C., Sandrolini, F., Andreola, F., Barbieri, L. and Lancellotti, I., 2010, June. Recycling electric arc furnace slag as unconventional component for building materials. *Proceedings of 2nd International Conference on sustainable construction materials and technologies*. Ancona, Italy , 557-567.
30. Adesanya, E., Sreenivasan, H., Kantola, A.M., Telkki, V.V., Ohenoja, K., Kinnunen, P. and Illikainen, M., 2018. Ladle slag cement-Characterization of hydration and conversion. *Construction and Building Materials*, *193*, 128-134. https://doi.org/10.1016/j.conbuildmat.2018.10.179
31. Arribas, I., Santamaria, A., Ruiz, E., Ortega-Lopez, V. and Manso, J.M., 2015. Electric arc furnace slag and its use in hydraulic concrete. *Construction and Building Materials*, *90*, 68-79. https://doi.org/10.1016/j.conbuildmat.2015.05.003
32. Choi, S., Kim, J.M., Han, D. and Kim, J.H., 2016. Hydration properties of ladle furnace slag powder rapidly cooled by air. *Construction and Building Materials*, *113*, 682-690. https://doi.org/10.1016/j.conbuildmat.2016.03.089
33. Coppola, L., Buoso, A., Coffetti, D., Kara, P. and Lorenzi, S., 2016. Electric arc furnace granulated slag for sustainable concrete. *Construction and Building Materials*, *123*, 115-119. https://doi.org/10.1016/j.conbuildmat.2016.06.142
34. González-Ortega, M.A., Cavalaro, S.H.P., de Sensale, G.R. and Aguado, A., 2019. Durability of concrete with electric arc furnace slag aggregate. *Construction and Building Materials*, *217*, 543-556. https://doi.org/10.1016/j.conbuildmat.2019.05.082
35. Faleschini, F., Fernández-Ruíz, M.A., Zanini, M.A., Brunelli, K., Pellegrino, C. and Hernández-Montes, E., 2015. High performance concrete with electric arc furnace slag as aggregate: mechanical and durability properties. *Construction and Building Materials*, *101*, 113-121. https://doi.org/10.1016/j.conbuildmat.2015.10.022.
36. Parron-Rubio, M.E., Perez-García, F., Gonzalez-Herrera, A. and Rubio-Cintas, M.D., 2018. Concrete properties comparison when substituting a 25% cement with slag from different provenances. *Materials*, *11*(6), 1029. https://doi.org/10.3390/ma11061029
37. Hekal, E.E., Abo-El-Enein, S.A., El-Korashy, S.A., Megahed, G.M. and El-Sayed, T.M., 2013. Hydration characteristics of Portland cement-Electric arc furnace slag blends. *HBRC Journal*, *9*(2), 118-124. https://doi.org/10.1016/j.hbrcj.2013.05.006

38. Amin, M.N., Khan, K., Saleem, M.U., Khurram, N. and Niazi, M.U.K., 2017. Influence of mechanically activated electric arc furnace slag on compressive strength of mortars incorporating curing moisture and temperature effects. *Sustainability*, *9*(8), 1178. https://doi.org/10.3390/su9081178
39. Adolfsson, D., Robinson, R., Engström, F. and Björkman, B., 2011. Influence of mineralogy on the hydraulic properties of ladle slag. *Cement and Concrete Research*, *41*(8), 865-871. https://doi.org/10.1016/j.cemconres.2011.04.003
40. Muhmood, L., Vitta, S. and Venkateswaran, D., 2009. Cementitious and pozzolanic behavior of electric arc furnace steel slags. *Cement and Concrete Research*, *39*(2), 102-109. https://doi.org/10.1016/j.cemconres.2008.11.002
41. Apithanyasai, S., Nooaek, P. and Supakata, N., 2018. The utilization of concrete residue with electric arc furnace slag in the production of geopolymer bricks. *Engineering Journal*, *22*(1), 1-14. https://doi.org/10.4186/ej.2018.22.1.1
42. Ozturk, M., Bankir, M.B., Bolukbasi, O.S. and Sevim, U.K., 2019. Alkali activation of electric arc furnace slag: Mechanical properties and micro analyzes. *Journal of Building Engineering*, *21*, 97-105. https://doi.org/10.1016/j.jobe.2018.10.005.
43. Hafez, H.; W. M. Cheung; B. Nagaratnam; R. Kurda. A proposed performance based approach for life cycle assessment of reinforced blended cement concrete. *Proceedings of the 5th SCMT conference*, Kingston University, UK, 2019, 50-61.
44. ASTM C33, 2003. ASTM C33 standard specifications for concrete aggregates. *ASTM Standard Book*.
45. NP EN 12350-2. Testing fresh concrete. Part 2: slump test. IPQ, Lisbon, Portugal; 2009. 11 p.
46. NP EN 12390-3. Testing hardened concrete. Part 3: compressive strength of test specimens. IPQ, Lisbon, Portugal; 2009. 21 p.
47. NT BUILD 492. 1991. Concrete, mortar and cement-based repair materials: Chloride migration coefficient from non-steady state migration experiments. Nordtest, Espoo, Finland.
48. L.N.E.C. E 391. 1993. Concretes: Determination of the carbonation resistance (in Portuguese), Lisbon, Portugal
49. Hafez, H., R. Kurda, W.M. Cheung, and B. Nagaratnam, A systematic review of the discrepancies of life cycle assessments of green concrete. *Applied Sciences*, 2019, ***9****(22)*, 4803. https://doi.org/10.3390/app9224803
50. Markeset, G. & Kioumarsi, M. 2017. Need for further development in service life modelling of concrete structures in chloride environment. *Procedia Engineering*, 171, 549-556. https://doi.org/10.1016/j.proeng.2017.01.37
51. Kurda, R., De Brito, J. & Silvestre, J. 2019. CONCRETop - A multi-criteria decision method for concrete optimization. *Environmental Impact Assessment Review*, 74, 73. https://doi.org/10.1016/j.eiar.2018.10.006